Human Molecular Genetics, 2003, Vol. 12, No. 17 **2179–2189**
DOI: 10.1093/hmg/ddg232

CRB1 is essential for external limiting membrane integrity and photoreceptor morphogenesis in the mammalian retina

Adrienne K. Mehalow[1,‡], Shuhei Kameya[1,‡,†], Richard S. Smith[1,‡], Norman L. Hawes[1,‡], James M. Denegre[1], James A. Young[1], Lesley Bechtold[1], Neena B. Haider[1], Ulrich Tepass[2], John R. Heckenlively[3], Bo Chang[1], Jürgen K. Naggert[1] and Patsy M. Nishina[1,*]

[1]The Jackson Laboratory, 600 Main Street, Bar Harbor, ME 04609, USA, [2]Department of Zoology, University of Toronto, Toronto, Ontario, Canada M5S 3G5 and [3]Jules Stein Eye Institute, Harbor-UCLA Medical Center, Torrance, CA 90095, USA

Received May 2, 2003; Revised June 27, 2003; Accepted July 5, 2003

Mutations within the *CRB1* gene have been shown to cause human retinal diseases including retinitis pigmentosa and Leber congenital amaurosis. We have recently identified a mouse model, retinal degeneration 8 (*rd8*) with a single base deletion in the *Crb1* gene. This mutation is predicted to cause a frame shift and premature stop codon which truncates the transmembrane and cytoplasmic domain of CRB1. Like in *Drosophila crumbs* (*crb*) mutants, staining for adherens junction proteins known to localize to the external limiting membrane, the equivalent of the zonula adherens in the mammalian retina, is discontinuous and fragmented. Shortened photoreceptor inner and outer segments are observed as early as 2 weeks after birth, suggesting a developmental defect in these structures rather than a degenerative process. Photoreceptor degeneration is observed only within regions of retinal spotting, which is seen predominantly in the inferior nasal quadrant of the eye, and is caused by retinal folds and pseudorosettes. Photoreceptor dysplasia and degeneration in *Crb1* mutants strongly vary with genetic background, suggesting that the variability in phenotypes of human patients that carry mutations in *CRB1* may be due to interactions with background modifiers in addition to allelic variations. The *Crb1^{rd8}* mouse model will facilitate the analysis of *Crb1* function in the neural retina and the identification of interacting factors as candidate retinal disease genes.

INTRODUCTION

Mutations in the *crumbs-like 1* (*CRB1*) gene lead to various forms of heritable retinal disorders in humans (1–5). CRB1 and related genes in other species encode transmembrane proteins that localize to the apical membrane of epithelial cells. The *Drosophila crumbs* (*crb*) gene has been studied extensively. Crb is a key regulator of polarity of many epithelial cells in which it acts as an apical determinant and contributes to the assembly of the zonula adherens (ZA), a belt-like adherens junction that separates apical and basolateral membranes (reviewed in 6).

Recent work has identified multiple roles for Crb in the *Drosophila* retina. Crb is essential for ZA integrity and for stalk membrane formation during the morphogenesis of photoreceptor cells (7,8). Primary defects in these structures cause a highly abnormal shape of photoreceptor cells, in particular, of the light sensing organelle, the rhabdomere. Moreover, Crb has also been shown to support photoreceptor survival during continuous light exposure (9). These findings suggest that CRB1 may be important for integrity of the ZA of the neural retina, also known as the external limiting membrane (ELM), and for the development of photoreceptor inner and outer segments, which are the subdivisions of the apical membrane

*To whom correspondence should be addressed. Tel: +1 2072886383; Fax: +1 2072886077; Email: pmn@aretha.jax.org
†Present address:
Department of Ophthalmology, Akita University School of Medicine, Akita 010-8543, Japan.
‡The authors wish it to be known that, in their opinion, the first four authors should be regarded as joint First Authors.

of photoreceptors that correspond to the fly stalk membrane and rhabdomere, respectively.

Interestingly, CRB1 mutations lead to a variety of retinal diseases including retinitis pigmentosa (RP) characterized by sparing of para-arteriolar retinal pigment epithelium (1), RP with Coats-like exudative vasculopathy (2) and Leber congenital amaurosis (LCA, 2–5). The retinal diseases observed cannot be explained solely by allelic differences as individuals with the same mutation have been reported to have different forms of RP (2). Multiple roles that CRB1 may play in retinal differentiation and maintenance, and its interaction with other cellular components necessary to carry out its function, might in part explain the range of retinal diseases and the variation in phenotype within each retinal disease observed. While much has been learned about *crb* function in *Drosophila*, a mammalian model would be extremely useful to begin to elucidate the causes of the broad spectrum of phenotypes observed in individuals with *CRB1* mutations.

RESULTS

Focal retinal dysplasia and degeneration with pan-retinal shortening of inner and outer segments is observed in *rd8* mice

During the process of introgressing *Mfrp*^{rd6} onto the C57BL/6 (B6) background, a mouse was found with large retinal spots rather than the usual, small, discrete, pan-retinally distributed spots. Through further crosses, we determined that a partial large spots phenotype could be produced in the absence of *Mfrp*^{rd6}, suggesting the presence of a second spontaneous mutation. This recessive mutation was named *retinal degeneration 8* (*rd8*).

Clinically, mice homozygous for the *rd8* mutation exhibit large, irregularly shaped spots most heavily concentrated in the inferior nasal quadrant of the fundus (Fig. 1). By orienting the eye prior to enucleation, we determined that the clinical spotting corresponds to regions with retinal folds and pseudorosettes that involve the photoreceptors and often distort the inner nuclear layer (Fig. 2B). Areas of retinal thinning that include both inner and outer segments are evident in affected regions. Unlike other models of photoreceptor degeneration that exhibit pan-retinal degeneration, degeneration in *rd8* mice is focal in nature. This aspect is particularly striking in older mice, in which the outer nuclear layer may be reduced to a single row of nuclei in a sharply demarcated area, with nearly normal retina present at the edge of the region of severe degeneration (Fig. 2C and D).

Electron microscopy reveals that the photoreceptor inner segments (PR IS), the equivalent of the *Drosophila* stalk membrane (7), also lose their orderly arrangement, and at 4 weeks of age are ~25% shorter than those of wild-type mice (Fig. 2E). This observation is consistent with findings in *Drosophila* (7), in which the lack of Crb leads to the formation of shortened stalks. Photoreceptor outer segments (PR OS) of *rd8* mutant mice are also shortened. By 10 weeks, outer segments begin to fragment, and a breakdown of individual photoreceptor lamellae is observed, resulting in the accumulation of granular debris (Fig. 2F). By 5 months, in the most affected regions, only a few outer segment fragments remain and the inner segments approach the retinal pigment epithelium. In addition, diffuse swelling of portions of the inner segments is observed (Fig. 2G). Although the inner retina is generally normal, Müller cell processes are unusually prominent both in the inner retina and in the inner nuclear layer. While normally difficult to identify, the Müller cell cytoplasm shows increased electron density and individual cytoplasmic strands that are easily traceable through the inner plexiform layer (Fig. 2H).

rd8 maps to chromosome 1 and is caused by a mutation in *Crb1*

Since *rd8* was first observed, 10 additional mouse strains have been identified that have retinal phenotypes similar to that of *rd8*. Complementation tests were carried out between B6.C3Ga-*rd8*/*rd8* and five of the strains; all of the retinal mutations were found to be allelic to *rd8*. Interestingly, all of the strains were incipient congenic strains in which different mutations were being introgressed onto the B6 background in our importation/induced mutant resource facility, suggesting a founder effect arising from a spontaneous mutation in the B6 strain.

To elucidate the molecular basis of *rd8* and to obtain a fine structure map for the locus, a mapping cross was produced by outcrossing B6.C3Ga-*rd8*/*rd8* and B6.FVB-*rd8*^{1J}/*rd8*^{1J} to CAST/EiJ, a wild-derived strain, and back-crossing the resulting F1 animals to an affected parent of the same strain (herein referred to as *rd8* and *rd8*^{1J} BC, respectively). The *rd8* locus was initially mapped by genome scan to mouse chromosome 1, ~73 cM from the centromere, in a cohort of 100 mice. The crosses were expanded to 339 back-cross progeny from the *rd8* BC and 267 back-cross progeny from the *rd8*^{1J} BC. All mice were phenotyped by indirect ophthalmoscopy and genotyped, initially with markers *D1Mit24* and *D1Mit42*, and subsequently with the flanking markers *D1Mit30* or *D1Mit498* proximally, and *D1Mit141* or *D1Mit423* distally (Fig. 3A). All mice recombinant within the critical interval were progeny tested to confirm whether the *rd8* mutation was being transmitted in the recombinant animal. Cumulatively, the critical interval containing *rd8* and *rd8*^{1J}, between markers *D1Mit538* and *D1Mt141*, was estimated to be 0.50 ± 0.29 cM.

Using mouse and human genome sequencing data, we assembled a physical contig across the minimal genetic region and found that it contained a mouse orthologue of the *Drosophila crb* gene (Fig. 3B). Sequence analysis of *Crb1* cDNA from *rd8* mice showed a one base pair deletion at nt3481, which causes a frameshift and a premature stop codon following amino acid 1207 (Fig. 3C). The entire coding region for *rd8*^{1J} was also tested for mutations by direct sequencing and the same nucleotide deletion was observed at nt3481. Subsequently, DNAs from the remaining strains with retinal spotting similar to that associated with *rd8* were tested by allele-specific PCR analysis and all strains harbored the same mutation. This finding supports the notion that the mutations observed in all of the incipient congenic strains were indeed caused by a C57BL/6 founder effect. The predicted mutant protein, if generated, would retain the EGF-like and LG-like domains, contain 47 novel amino acids following amino acid 1160 and end prior to the transmembrane domain of the CRB1 protein (Fig. 3D). From hereon, we will refer to the *rd8* mutation as *Crb1*^{rd8}.

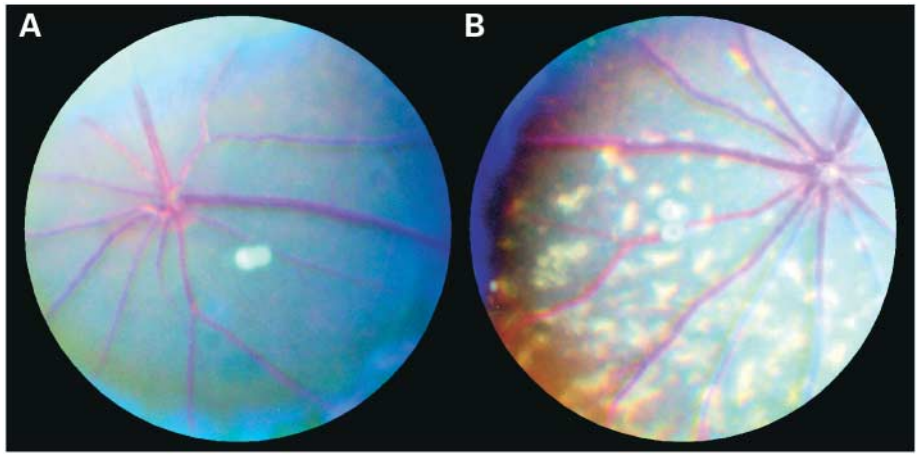

Figure 1. Fundus photographs of C57BL/6 and B6.C3Ga-*Crb1*^{rd8}/*Crb1*^{rd8} mutant mice. (**A**) Normal, control. (**B**) Homozygous *Crb1*^{rd8}/*Crb1*^{rd8} mouse exhibiting multiple intraretinal spots localized to the inferior nasal quadrant of the fundus. The white, irregularly shaped spots are detectable as early as 3 weeks of age.

The external limiting membrane is disrupted in *Crb1*^{rd8} mutants

crb loss-of-function mutants in *Drosophila* do not establish normal ZAs in photoreceptors (7,8). To determine if loss of CRB1 in mouse eyes affects ELM/ZA integrity, a number of proteins that localize to the ELM were examined in *Crb1*^{rd8}/*Crb1*^{rd8} mice. As others have shown, antibodies against ZO-1, ß-catenin, p120ctn, and pan-cadherin strongly stain the ELM of the neural retina of WT mice (Fig. 4A and D and data not shown) (10). Fragmented staining of the ELM with all markers was observed in *Crb1*^{rd8}/*Crb1*^{rd8} mice (Fig. 4B, C, E and F and data not shown), even in areas that were not affected by folds and pseudorosettes (Fig. 4C and F).

In order to determine when the abnormalities in the ELM/ZA were first observed, we also examined retinas from 2-week old mice. At this stage of retinal development, all of the retinal layers are present, although some remodeling is still occurring, and the PR IS are formed but the PR OS have yet to reach their adult length (11). Unlike the retinas of 4-week old *Crb1*^{rd8} mice, in which the fragmented ELM was observed pan-retinally, in retinas of 2-week old mice only the posterior ELM was affected (Fig. 4H). A linear, uninterrupted ELM was observed peripherally in *rd8* mice (Fig. 4G) and pan-retinally in WT 2-week old mice. Interestingly, the fragmentation and disorganization of the ELM appeared to be more severe in the 2- versus 4-week old retinas.

The aberrant staining pattern of the ELM was confirmed as a loss of adherens junctions by electron microscopy. Adherens junction complexes are considerable distances apart in *Crb1*^{rd8}/*Crb1*^{rd8} mice (Fig. 5B and D) in comparison with wild-type mice (Fig. 5A–C). A focal expansion of the extracellular space, which contains amorphous granular material, or of photoreceptor cell bodies is observed in regions where the ZA is absent in *Crb1*^{rd8}/*Crb1*^{rd8} mice (Fig. 5E). Furthermore, Müller cell apical processes were not observed immediately beneath the regions that did not contain adherens junctions, suggesting a developmental anomaly or retraction of the apical processes of the Müller cells from the ELM region. This correlated with absent or reduced staining of the Müller cell apical processes by antibodies against CD44 (Fig. 6E and F), an adhesion receptor that localizes only within these processes (10).

CRB1 localizes to Müller cells and photoreceptor inner segments

To determine the effect of the mutation of *Crb1* on CRB1 protein level and localization in *Crb1*^{rd8}/*Crb1*^{rd8} mice, immunohistochemical studies were carried out. Using polyclonal antibodies raised against synthetic peptides from the extracellular domain of CRB1 (amino acids 423–437 and 586–602), we observed the highest intensity staining of the Müller cell radial processes in the inner nuclear layer (INL) and in apical processes sclerad to the ELM, and of photoreceptor inner segments (Fig. 6A). Our results differ from those of Pellikka *et al.* (7), who also reported staining in cone photoreceptor outer segments in wild-type mice. That nine of 10 peptide residues used to raise the polyclonal CRB1 antibody used by Pellikka *et al.* (7) were identical to a sequence from a related protein, CRB2, suggests the potential for cross-reactivity. In mice homozygous for the *Crb1*^{rd8} mutation, CRB1 staining in the apical processes of the Müller cell was absent or diffuse (Fig. 6A and B); however, staining of the inner segment appeared the same in both mutant and wild-type retinas. This suggests that the transmembrane and/or cytosolic domain of *Crb1* is important for the localization of CRB1 to the apical processes of the Müller cells. Consistent with this view, MPP5 (also known as PALS1), the mammalian homolog of the *Drosophila* gene, *stardust* (12,13), whose product has been shown to interact directly with Crumbs1 (14), was also absent or showed a diffuse staining pattern in the ELM region in *rd8* mice (Fig. 6C and D). We note that the outer plexiform layer was brightly stained, and that the apparent localization and intensity of this staining was not affected in *rd8* mutants.

Alternative splice variants of *Crb1*

The absence of CRB1 staining of the Müller cell apical processes in the *Crb1*^{rd8} mutants, and the continued staining of IS, suggested the existence of splice variants that did contain

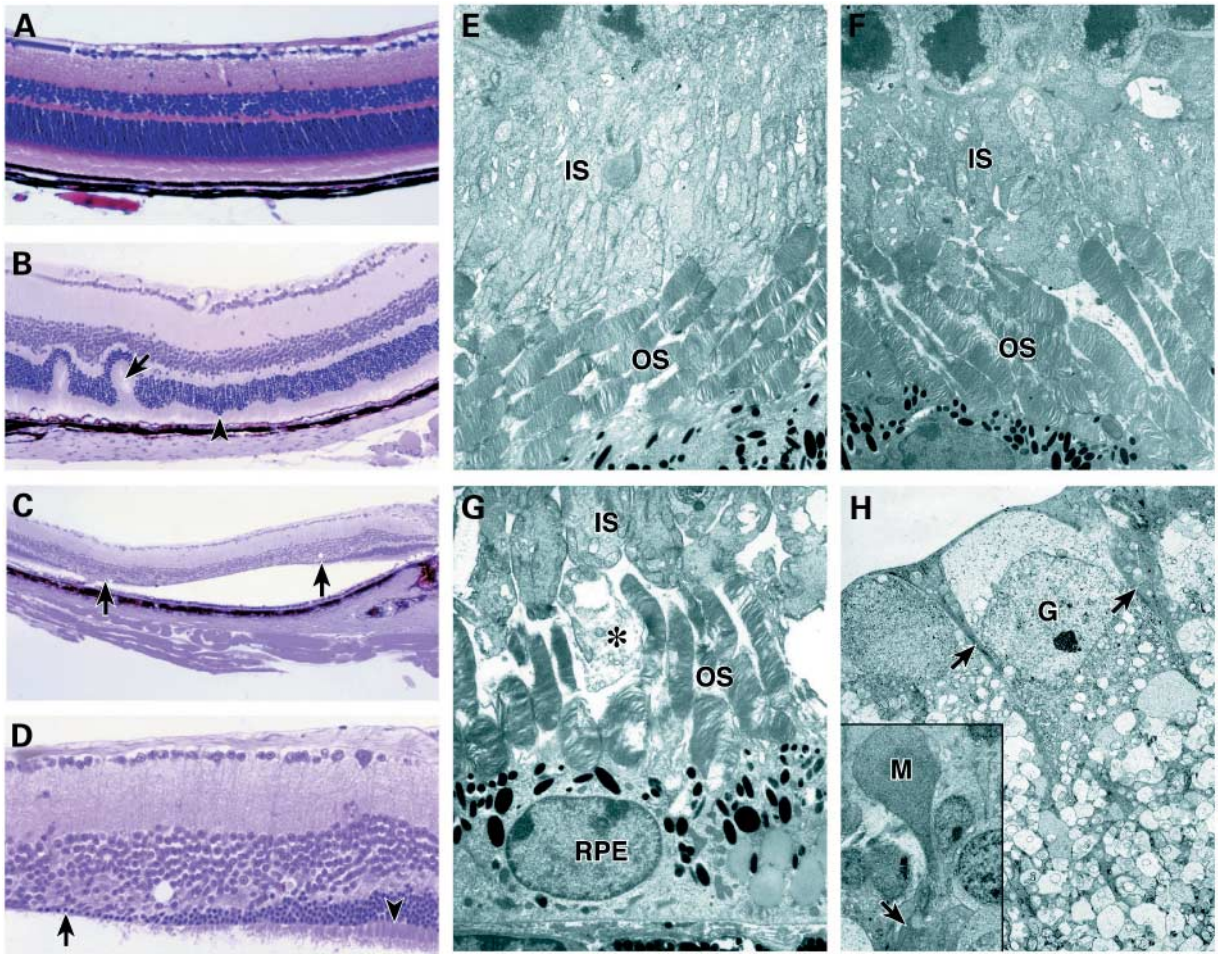

Figure 2. Retinal dysplasia and degeneration of photoreceptors in wild-type, control (A) and *Crb1*^{rd8}/*Crb1*^{rd8} mice visualized by light microscopy (B–D) and by electron microscopy (E–H). (**A**) Retina from 4-week-old C57BL/6 mouse. (**B**) At 4 weeks, most of the retinal architecture is normal. There are occasional retinal folds, involving inner and outer nuclear layers (arrow). There is also focal thinning of the inner and outer segments (arrowhead). (**C**) Focal photoreceptor degeneration, demarcated by arrows, is observed with mouse age (specimen from a 35-month-old mouse). In the degenerated region, the outer nuclear layer is reduced to a single row of nuclei and both inner and outer segments are absent. (**D**) The region of focal degeneration at higher magnification shows a prominent loss of the photoreceptors, which in places are reduced to a single layer of nuclei (arrow). Near this area of severe degeneration, nearly normal retinal architecture is preserved including normal inner and outer segments (arrowhead). Hematoxylin and eosin. Magnification: (A) ×200; (B) × 200; (C) ×100; (D) ×400. (**E**) By electron microscopy, at 4 weeks of age a shortening of both inner and outer segments is noted. (**F**) At 10 weeks of age there is inner segment shortening and outer segment disorganization. In both D&E, the inner segments are approximately one-quarter to one-third normal length. (**G**) At 5 months of age there are only a few short fragments of outer segments (OS). Some inner segments (IS) appear normal while others (asterisk) are swollen. (**H**) The cytoplasm of Muller cells of the inner retina is more prominent in *Crb1*^{rd8}/*Crb1*^{rd8} mice than normal (specimen from an 8-week-old mutant); two Müller cell processes are indicated by arrows. Inset: a Müller cell body (M) in the inner nuclear layer and its cytoplasmic processes (arrow) are also unusually prominent. (D) and (E) original magnification ×8100; (F) and (G) ×12 000; inset ×8100.

the exon 6-encoded epitope for the polyclonal antibodies but not exon 9, which is mutated in *Crb1*^{rd8} mice. Database searches with the genomic *Crb1* DNA sequence identified the ESTs BB642749 and AW491657, from a retinal and a pineal library, respectively, which were derived from a novel, shorter *Crb1* splice variant (B in Fig. 7). This splice variant utilizes a novel 5′ exon located in intron 5 which contains an ATG start codon with upstream in-frame stop codons. The putative amino terminal sequence is conserved in a human EST (BM687886, 76% similarity/53% identity over 17 amino acid residues), which also has upstream in-frame stop codons. This splice variant also utilizes an alternate polyadenylation site located in intron 11. The presence of this splice form in retinal mRNA was confirmed by sequencing of PCR products obtained from retinal cDNA using primers derived from the 5′ non-coding region of exon 5a and intron 11 within the alternate 3′ non-coding region of splice form B. The deduced amino acid sequence lacks the transmembrane domain of the full-length CRB1 splice form A, which is encoded by exon 12. Since the amino terminal sequence of splice form B also lacks a signal sequence, we predict that CRB1 isoform B is localized intracellularly. PCR amplification of retinal cDNA with combinations of primers obtained from all exon sequences yielded additional products that lack individual exons, indicating that additional splice variants may exist (Fig. 7C–G). However, all of the full length splice variants that we were able to amplify contained exon 9.

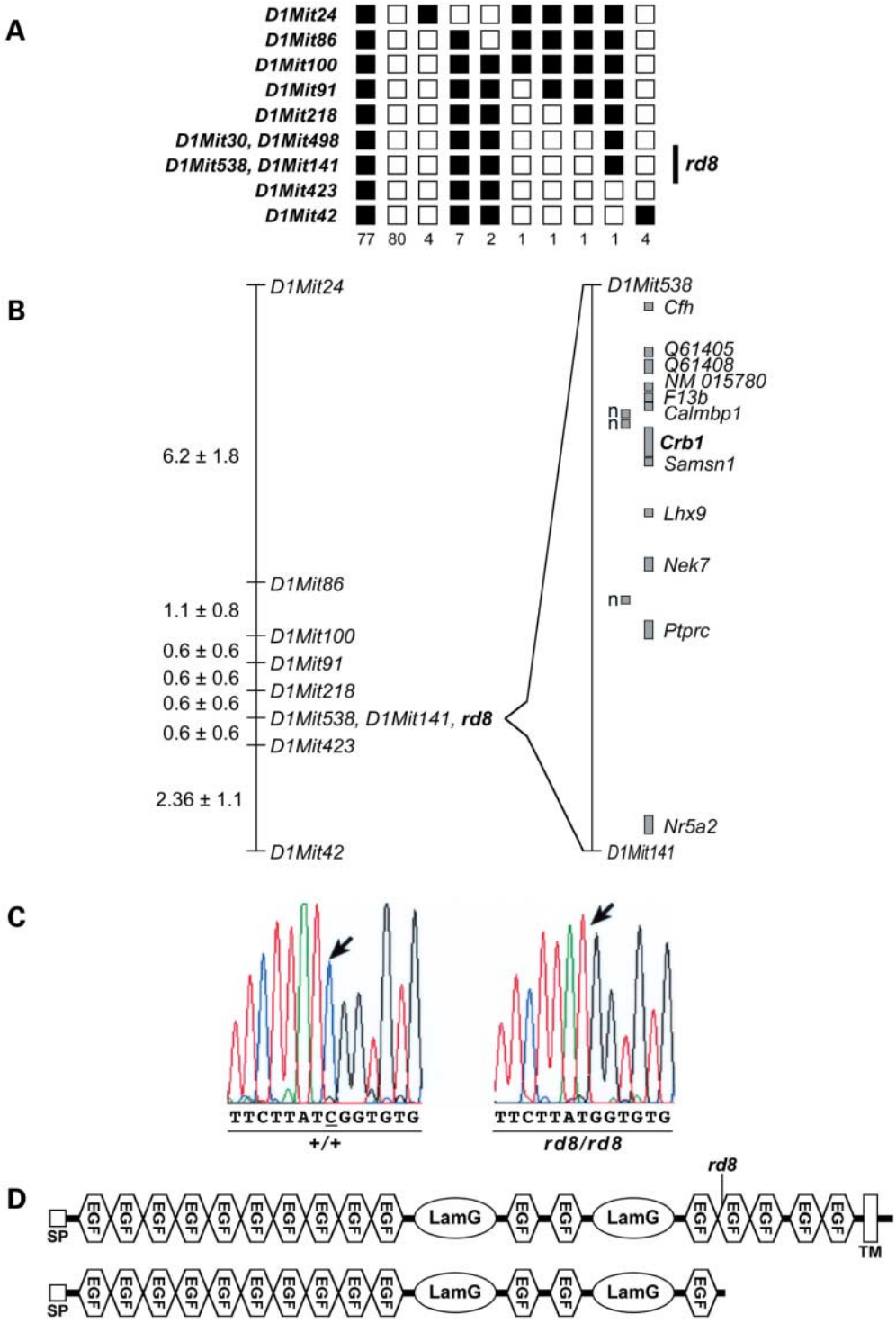

Figure 3. Genetic and molecular analysis of the *rd8* mutation. (**A**) Haplotype analysis. Progeny from the (B6.C3Ga X CAST-*rd8*/+)F1 X B6.C3Ga-*rd8/rd8* or (B6.FVB X CAST-$rd8^{1J}$ /+)F_1 × B6.FVB-$rd8^{1J}$ /$rd8^{1J}$ back-cross were phenotyped for the retinal spotting phenotype and genotyped for the indicated microsatellite markers. Black boxes represent heterozygosity, B6 and CAST-derived alleles and white boxes represent homozygosity for the B6-derived allele. The number of chromosomes sharing the corresponding haplotype is indicated below each column of squares. The order of marker loci was determined by minimizing the numbers of crossovers. The genotype for *rd8* was inferred from the phenotype or the results of progeny testing of non-informative recombinants. (**B**) Chromosomal map position of *rd8*. A total of 606 BC progeny was typed with markers listed left of the vertical lines representing the region identified as containing *rd8* on chromosome 1. The recombination frequencies are given in centimorgans ± SE. On the right hand of the vertical line is a transcript map of the *rd8* minimal region. 'n' represents novel uncharacterized genes. (**C**) A deletion of nt 3481 of the *Crb1* cDNA, a cytosine, is observed in *rd8* mice but not wild-type controls. The arrow indicates the deleted nucleotide. (**D**) Schematic of protein truncations. Wild-type CRB1 protein contains a signal peptide (SP), 17 epidermal growth-factor-like domains, three laminin A G-like domains, and a transmembrane (TM) domain. If translated, the mutant mRNA in *rd8* mice would produce a protein that does not contain the transmembrane or cytosolic domains of CRB1.

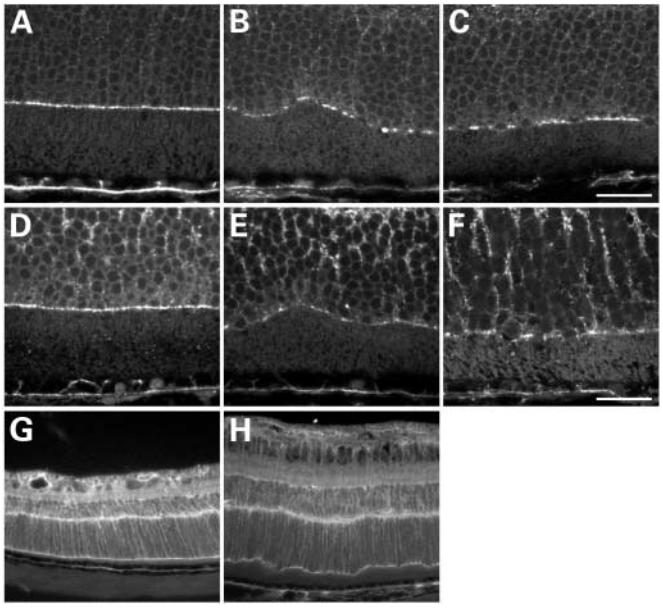

Figure 4. Aberrant ELM staining with anti-adherens junction markers in *Crb1*^{rd8}/*Crb1*^{rd8} mice. (A–F) Retinal specimens from 4-week-old mice; (G, H) retinal specimens from 2-week-old mice. (A–C) Stained with anti-ß-catenin; (D–H) stained with anti-pancadherin. In comparison to wild-type controls (**A, D**) in which linear staining is observed across the ELM, *Crb1*^{rd8}/*Crb1*^{rd8} mice show fragmented, discontinuous staining both in regions affected by retinal folds and pseudorosettes (**B, E**) and in unaffected regions (**C, F**). In 2-week-old mice, discontinuous, fragmented ELM staining is observed only in the posterior retina (**H**) and not in the peripheral retina (**G**). (A–F) Scale bars are 20 µm; (G–H) original magnification ×20.

Suppression of retinal spotting and dysplasia observed in *Crb1*^{rd8}/*Crb1*^{rd8} mutants

Observation of *Crb1*^{rd8} homozygotes from the mapping cross to the wild-derived CAST/EiJ mice revealed that the degree of the spotting phenotype is highly variable. While parental *Crb1*^{rd8}/*Crb1*^{rd8} mice have a relatively uniform spotting phenotype in the inferior nasal quadrant of the eye, *Crb1*^{rd8} homozygotes on the segregating CAST/EiJ background have many more or fewer spots. In fact, we noted 19% of mice that were homozygous for the mutation in *Crb1* did not exhibit the retinal spotting phenotype. In addition, during the process of introgressing the *Crb1*^{rd8} mutation onto the C57BL/6J background, the retinal spotting was no longer evident by indirect ophthalmoscopy at back-cross generation N7. Therefore, it appears that genetic modifiers exist that are able to suppress as well as enhance the degree of retinal spotting.

Retinal folds or pseudorosettes were not observed in histological sections of retinas from mice that were homozygous for the *Crb1* mutation and suppressed for the clinical retinal spotting phenotype. Gross histological examination of retinas from suppressed *Crb1*^{rd8}/*Crb1*^{rd8} mice was essentially normal without shortening and disorganization of the inner and outer segments. However, the anti-ZA markers tested on retinas of suppressed mice revealed a discontinuous, fragmented staining pattern similar to that observed in non-suppressed *Crb1*^{rd8}/*Crb1*^{rd8} mice (Fig. 8), suggesting that retinal folding and photoreceptor inner segment shortening and disorganization are

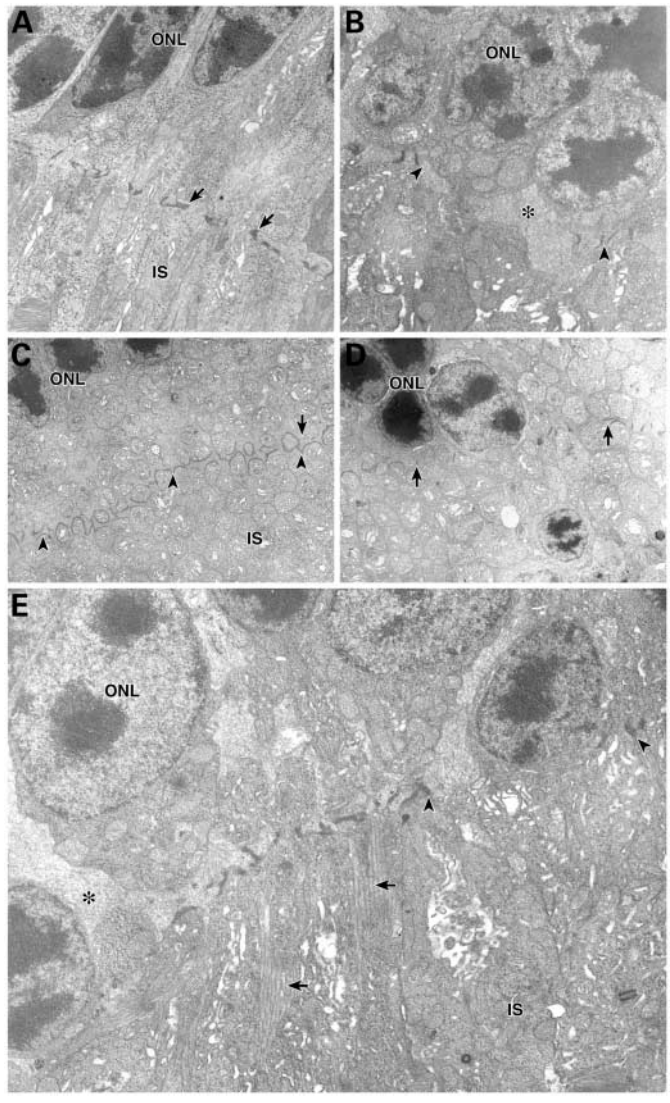

Figure 5. Aberrant ELM staining with anti-adherens junctional (AJ) markers is due to a reduction in AJ complexes. (**A**) In a normal, wild-type mouse (4 weeks), the external limiting membrane is composed of complexes of adherens junctions (arrows) that are present between Müller cells–photoreceptors, Müller cells–Müller cells, and photoreceptor–photoreceptors. The individual AJ are arranged in linear fashion without interruption. There is no visible extracellular space at the level of the external limiting membrane. (**B**) In *Crb1*^{rd8}/*Crb1*^{rd8} mutants (4 weeks), AJ complexes are absent for considerable distances (delimited by arrowheads). Where these elements are absent, there is focal expansion of the extracellular space (asterisk), which contains amorphous granular material. The photoreceptor inner segments (IS) have lost the orderly arrangement of those in (A). The continuous nature of the external limiting membrane (arrowheads) is demonstrated in *en face* section of retinas from wild-type controls (**C**). The cytoplasm of Müller cells (arrow) sectioned *en face* is more easily identified than in cross sections. When the angle of section is appropriate, circular profiles of inner segments are encircled by adherens junctions joining them to the Müller cells. (**D**) Extensive sections of the external limiting membrane are absent in *Crb1*^{rd8}/*Crb1*^{rd8} mice (delineated by arrows) in *en face* sections of external limiting membrane region. There is less Müller cell cytoplasm than is seen in the wild-type mouse. (**E**) The villous extensions of the Muller cells (arrows) sclerad to the external limiting membrane are clearly seen where the AJ are present in *Crb1*^{rd8}/*Crb1*^{rd8} mutant retina. Gaps in the external limiting membrane (delineated by arrowheads) are generally filled with photoreceptor cell bodies, and Müller cell processes are missing in these regions. Swollen Müller cell cytoplasm (asterisk) is present in the ONL. (A–D) Original magnification ×20 100; (E) original magnification ×12 000.

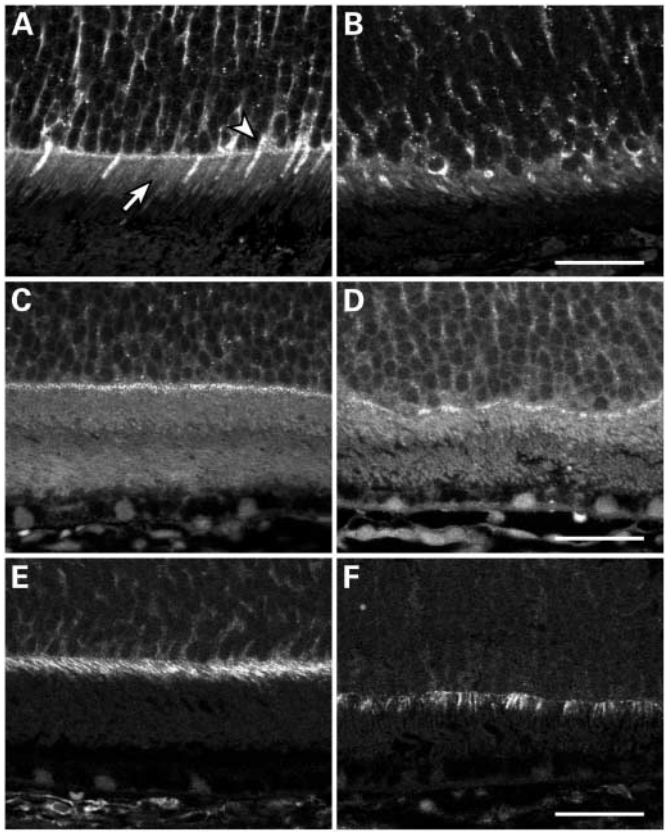

Figure 6. CRB1, PALS1 and CD44 staining is absent or diffuse in the apical processes of the Müller cells of the *rd8* mutant retina. In C57BL/6, wild-type controls (**A**) anti-CRB1 staining is observed in the radial processes in the inner nuclear layer and the apical processes of Müller cells (white arrowhead) and in photoreceptor inner segments (arrow). (**B**) In comparison, while overall staining of the Müller cells does not seem significantly different from WT controls, staining of Müller cell apical processes is absent in $Crb1^{rd8}/Crb1^{rd8}$ mice. Inner segment staining is similar or somewhat reduced in *rd8* mice compared to controls. (**C**) PALS1, a factor that is known to interact directly with CRB1, showed significant staining in the inner plexiform layer and in the region apical to the ELM in wild-type controls. (**D**) Anti-PALS1 staining is absent or diffuse in the ELM region. (**E**) In wild-type controls, anti-CD44 staining is present in the apical processes of Müller cells. (**F**) In comparison, anti-CD44 staining is patchy. (A–F) Scale bars are 25 μm.

secondary phenotypic changes that are controlled by genes other than *Crb1*.

Crossing suppressed B6.Cg-$Crb1^{rd8}/Crb1^{rd8}$ mice (N10F3) with non-suppressed B6.C3Ga-$Crb1^{rd8}/Crb1^{rd8}$ mice (N3F12), yielded offspring ($n = 18$) of which 100% were observed to have retinal spots. This suggests that the factor(s) necessary for the retinal dysplasia acts in a dominant fashion and is probably a contribution from C3HfB6/Ga (15).

DISCUSSION

The defects observed in $Crb1^{rd8}$ mutant mice show striking similarities to those caused by *crb* mutations in the *Drosophila* retina (7,8). As in *Drosophila crb* mutants, the ELM/ZA is fragmented, and the ZA defects are more severe in the developing retina compared to the mature retina in $Crb1^{rd8}$ mutants (7). In $Crb1^{rd8}/Crb1^{rd8}$ mice, the loss of ELM integrity was more notable at 2 than at 4 weeks, particularly in the posterior retina; this appears to be coincident with the posterior to peripheral maturation and migration of the photoreceptors (16). In the mature $Crb1^{rd8}$ mutant retina, photoreceptor cell bodies protrude into the inner segment layer. Previous studies have suggested that the ELM provides a barrier function, as mice having a chemically induced deficiency of retinal Müller cells, which form ZAs with photoreceptors, exhibit mislocalized photoreceptor cell bodies in the inner and outer segment layers (17).

The $Crb1^{rd8}$ mutation truncates the transmembrane and cytoplasmic domain of the CRB1 protein suggesting that it may produce a secreted protein that consists of most of the extracellular domain of CRB1. Overexpression of the extracellular domain of *Drosophila* Crb has a dominant-negative effect on the formation of the stalk membrane (7). We have observed retinal defects only in homozygous mutant $Crb1^{rd8}$ animals but not in heterozygous animals. This may imply that either the secreted, extracellular domain of CRB1 has no dominant-negative effect, or that the expression from the endogenous CRB1 promoter is not producing sufficient gene product to cause phenotypic consequences. *Drosophila* Crb presumably plays mechanistically distinct roles in the formation of the ZA and the stalk membrane (7,8). Whether both of these roles have been conserved in the mammalian retina remains to be clarified. For example, current evidence is consistent with the view that the primary role of CRB1 is the maintenance of the ELM/ZA and that the shortening of the inner segment is a secondary consequence of the fragmented ELM/ZA observed in Crb^{rd8} mutants. To identify conserved and potentially novel roles of CRB1 in the mammalian retina, it will be important to characterize the network of factors that interact with CRB1 in retinal development.

A recent publication, in which retinas of individuals diagnosed with LCA and harboring *CRB1* mutations were examined by optical coherence tomography, reports thickened retinas with abnormal lamination and photoreceptor rosettes (18). Although we observed retinal folds and pseudorosettes in B6.C3Ga-$Crb1^{rd8}/Crb1^{rd8}$ mice, the retinal architecture was, in general, normal. Only within the dysplastic regions were abnormalities in lamination, involving both the INL and ONL, observed. The discrepancy in phenotypic features observed in the retina between mice and humans could be potentially explained by allelic or by species differences. The former explanation may be less likely given the fact that the thickening and abnormal lamination of the retina were observed in individuals with mutations throughout *Crb1*, including the region predicted to be truncated in the *rd8* mutant (Fig. 9) (18). Previous reports, showing species differences in retinal disease manifestation have been reported, for example, in shaker mice, which harbor a mutation within myosin VIIA (19). In humans, mutations within myosin VIIA lead to both hearing and vision loss in patients with Usher Syndrome Type 1B (20), while shaker mice only develop hearing loss. This is presumably due to species differences in the localization of the protein within the retina (21,22). It is also possible that the difference in clinical features found between humans and our mouse model, and the relatively mild retinal disease observed in $Crb1^{rd8}$ mutant mice, may be due to the genetic background in which the $Crb1^{rd8}$ mutation currently resides.

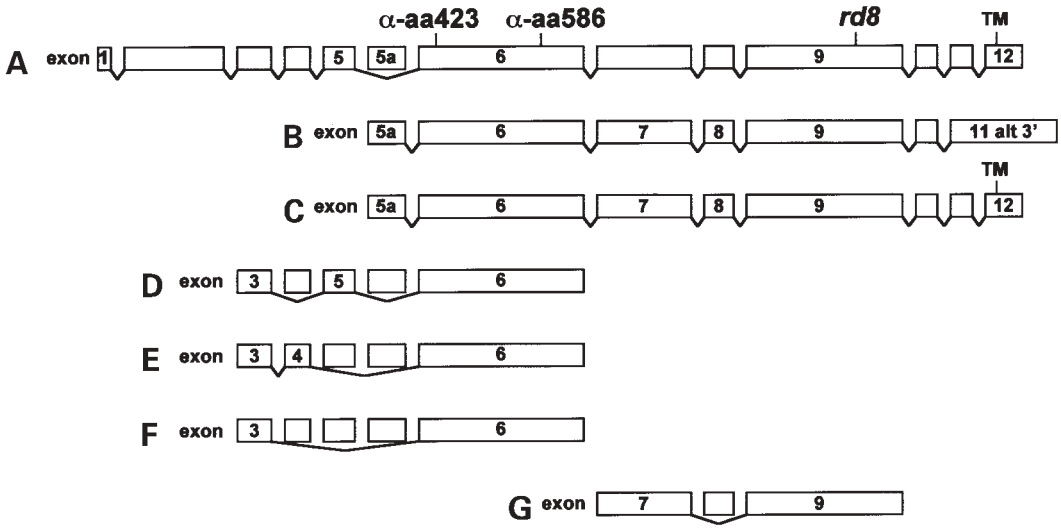

Figure 7. Multiple alternative splice variants of *Crb1* are observed in the retina. Presented are schematics of splicing variants observed in *Crb1* transcripts. Introns are not drawn to scale. Exons, the transmembrane domain, and the positions of the *rd8* mutation and the sequences used to generate peptide antibodies are indicated. The long form of *Crb1* (splice variant A) has been reported previously (25). Splice variants (**A**–**C**) are the prominent products obtained by PCR amplification of retinal cDNA using primers located in the 5′ and 3′ non-coding regions of the respective transcripts. Splice products (**D**–**G**) were obtained by inter-exon amplification of retinal cDNA; the full-length sequence of these forms is not known.

Perhaps the most interesting observation of $Crb1^{rd8}/Crb1^{rd8}$ mice, which sheds light on the variability in clinical features observed in individuals with CRB1 mutations, is that genetic modifiers are able to determine the severity of the disease phenotype. Den Hollander *et al.* (2) suggested that the wide range of phenotypic characteristics observed in individuals with *CRB1* mutations could be due to environmental or genetic factors. We provide evidence that genetic factors do indeed influence the disease phenotype in the presence of a $Crb1^{rd8}$ mutation. The fact that retinal degeneration is not observed in $Crb1^{rd8}/Crb1^{rd8}$ mice suppressed for retinal dysplasia suggests that, in mice, *Crb1* may be thought of as a susceptibility locus whose mutant form must interact with mutant/variant alleles at other loci for disease to manifest. Additional studies using different inbred strains may help to identify factors contributing to the retinal dysplasia and to clarify the apparent differences in the presentation of retinal histology in humans and mice carrying *Crb1* mutations. Also, such genetic modifier screens may further define the molecules involved in the function of CRB1 and should identify candidate retinal disease genes.

MATERIALS AND METHODS

Mice

Mice were bred and maintained under standard conditions in the Research Animal Facility at The Jackson Laboratory. They were maintained on NIH 4% fat chow and acidified water, with a 12 : 12 hour dark : light cycle in facilities that are monitored regularly to maintain a specific pathogen-free environment. Procedures used in the experiments were approved by the Institutional Animal Care and Use Committee. B6.C3Ga-*rd8*/*rd8* (N3F12) and B6.FVB-$rd8^{1J}/rd8^{1J}$ (N4F9) were used in the initial mapping crosses with CAST/EiJ mice. B6.Cg-*rd7*/+;*rd8*/*rd8* (N10F3) and B6.C3Ga-*rd8*/*rd8* (N3F12) were used for the suppressor and phenotypic studies.

Chromosomal localization and fine structure mapping

Tail DNA was isolated from mice generated by backcrosses described above according to Buffone and Darlington (23). DNAs of the 606 BC offspring were genotyped using microsatellite markers to develop a fine structure map of the region. Critical recombinant mice were progeny tested by crossing them to F2(B6.C3GaXCAST) *rd8*/*rd8* mice to confirm informative recombinants or to determine if a presumed uninformative recombinant carried the disease gene. A minimum of 20 offspring from each progeny test were genotyped and phenotyped. For PCR amplification, 25 ng DNA was used in a 10 µl volume containing 50 mM KCl, 10 mM Tris–Cl, pH 8.3, 2.5 mM $MgCl_2$, 0.2 mM oligonucleotides, 200 µM dNTP, and 0.02 U AmpliTaq DNA polymerase. The reactions which were initially denatured for 2 min at 95°C were subjected to 49 cycles of 20 s at 94°C, 20 s at 50°C, 30 s at 72°C and a 7 min extension at 72°C. PCR products were separated by electrophoresis on a 4% MetaPhor (FMC, Rockland, ME, USA) agarose gel and visualized under UV light after staining with ethidium bromide.

Clinical examination of eyes

Mice were dark adapted and their pupils dilated with atropine prior to examination by indirect ophthalmoscopy with a 78 or 90 diopter aspheric lens. Fundus photographs were taken with a Kowa fundus camera using a Volk superfield lens held two inches from the eye. The highest flash intensity was used with 400ASA film for the photodocumentation.

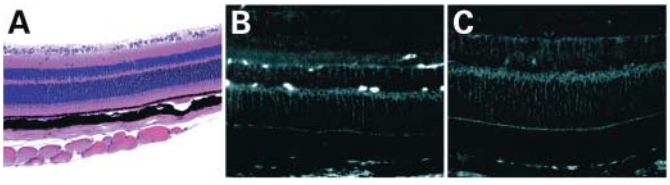

Figure 8. Genetic modification of the retinal phenotype in mice homozygous for *Crb1*^{rd8} and segregating on a C57BL/6 and C3H genetic background. (**A**) Suppressed *Crb1*^{rd8}/*Crb1*^{rd8} mice do not exhibit retinal folds or pseudorosettes. Even at 11.5 months, the general architecture of the suppressed *rd8* retina is normal. The shortening of the inner and outer segments observed in *Crb1*^{rd8}/*Crb1*^{rd8} mice is not evident in suppressed mice. Staining of the ELM with anti-adherens junction markers of suppressed *Crb1*^{rd8}/*Crb1*^{rd8} mice (**B**) and age-matched wild-type controls (**C**) shows that the adherens junctions are discontinuous and fragmented, but not as severely as observed in non-suppressed *Crb1*^{rd8}/*Crb1*^{rd8} mice.

Histological analysis

Light microscopy. Eyes were oriented by marking the cornea by cauterization, after sacrifice but prior to enucleation, and were placed in Bouin's fixative or acetic acid : methanol (1 : 3) overnight, embedded in paraffin, and sectioned in a plane that included the ora serrata and optic nerve. Sections were stained with hematoxylin and eosin.

Electron microscopy. The eyes were removed immediately after carbon dioxide euthanasia of each mouse and fixed for 3 h in a cold, phosphate-buffered, glutaraldehyde–paraformaldehyde solution. After 3 h, the anterior segment was removed and the posterior segment cut into 1 × 2 mm blocks of retina, choroid and sclera. The additional fixation of the whole eye before dissection improved adhesion of the retina to the retinal pigment epithelium (RPE) and did not alter the quality of preservation. The dissected tissue was placed in fresh fixative for an additional 2–8 h and was post-fixed in 1% osmium tetroxide, dehydrated and embedded in plastic. Thick sections were cut for orientation and thin sections cut and stained with uranyl acetate and lead citrate and examined using a transmission electron microscope.

Immunohistochemistry. Mice homozygous for the *rd8* mutation and wild-type controls were sacrificed by cervical dislocation or carbon dioxide asphyxiation. Enucleated, oriented eyes were fixed with either acetic acid : methanol (1 : 3) or 4% paraformaldehyde (PFA) in phosphate-buffered saline (PBS) overnight prior to embedding in paraffin. For mutants and for controls, a minimum of three eyes, each from a different animal, were tested with each primary antibody. Sections of 6 µm thickness were cut and mounted on slides pretreated with Vectabond (Vector Laboratories, Burlingame, CA, USA). After blocking with 2% normal horse serum in PBS, sections were incubated overnight with primary polyclonal antibodies for zonula occludens-1 (1 : 200; Zymed, South San Francisco, CA, USA), p120 catenin (1 : 200; Santa Cruz Biotechnology Inc., Santa Cruz, CA, USA), CRB1 (1 : 100), CRB2 (1 : 200), and monoclonal antibodies for pan cadherin (1 : 200; Sigma, St Louis, MO, USA), β-catenin (1 : 200; Santa Cruz Biotechnology Inc., Santa Cruz, CA, USA) and CD44 (1 : 200; Research Diagnostics, Flanders, NJ, USA). Polyclonal antibodies against PALS1 were provided by Dr B. Margolis (14) and used at a 1 : 200 dilution. Secondary antibodies were biotin-conjugated anti-rabbit IgG (1 : 200, Vector Laboratories) for zonula occludens-1, CRB1, CRB2, and PALS1, biotin-conjugated anti-goat IgG (1 : 200, Vector Laboratories) for p120 catenin, biotin-conjugated anti-mouse IgG (1 : 200 Vector Laboratories) for pan-cadherin and β-catenin, and biotin-conjugated anti-rat IgG (1 : 200, Vector Laboratories) for CD44. Binding was detected using FITC-Avidin D (1 : 200, Vector Laboratories). Nuclear counterstaining was performed with 4,6 diamidine 2-phenylindoledihydrochloride (DAPI) at a final concentration of 5 µg/ml. Images were collected on a Leica DMRXE fluorescent microscope (Leica, Deerfield, IL, USA) equipped with a SPOT™ CCD camera (Diagnostic Instruments, Sterling Heights, MI, USA) using appropriate band-pass filters for each fluorochrome, or on a Leica TCS NT confocal microscope (Leica, Deerfield, IL, USA) using a 40 × 0.85 NA lens or a 100 × 1.25 NA oil immersion lens. Appropriate band-pass filters for each fluorochorome were used and image collection was optimized to fill the 256 gray levels available.

Generation of the CRB1 and CRB2 polyclonal peptide antibodies

Polyclonal CRB1 anti-peptide antibodies were generated in rabbit by Peptide Specialty Laboratories GmbH (Heidelberg, Germany). Peptides corresponding to amino acids 423–437 (PFDDTSRTFYGGENC) and 586–602 (CKEKCTTKSSVPV-ENHQ) were synthesized, coupled to KLH and used to immunize two rabbits. Sera were tested by ELISA after three immunizations, with positive results. After collection, aliquots of sera were affinity-purified against both peptides conjugated to SulfoLink Coupling Gel®, according to the manufacturer's protocols (Pierce Biotechnology, Rockford, IL, USA). Preimmune sera, immune sera, and affinity-purified sera were all tested by immunocytochemistry against target tissue. Preimmune sera showed no staining of tissue.

Anti-CRB2 polyclonal antibody were generated in a rabbit immunized with a CRB2 peptide (aa941-955) coupled to keyhole limpet hemocyanin and was peptide affinity purified (Sigma-Genosys, The Woodlands, TX, USA).

Mutation analysis of *Crb1* and identification of alternative splice factors

Total RNA was isolated from whole eyes of B6.C3Ga-*rd8/rd8*, B6.FVB-*rd8*^{1J}/*rd8*^{1J} and C57BL/6J mice. Tissues were homogenized and RNA was isolated by TRIzol (Life Technologies) treatment according to the manufacturer's protocol. cDNA was generated using the Retroscript kit (Ambion). Primers to detect splice variants of *Crb1* were designed from exons or EST sequences obtained from GenBank or Celera databases. PCR assays were carried out using the Expand Template system (Roche) and gel purified amplicons were sequenced with an ABI Prism 3700. Allele-specific PCR (24) was used on genomic DNA to confirm the presence of the *rd8* mutation using the primers: mCrb1-mF1 GTGAAGACAGCTACAGTTCTGATC; mCrb1-mF2, GCCCCTGTTTGCATGGAGGAAACTTGGA-AGACAGCTACAGTTCTTCTG; and mCrb1-mR, GCCCCA-TTTGCACACTGATGAC.

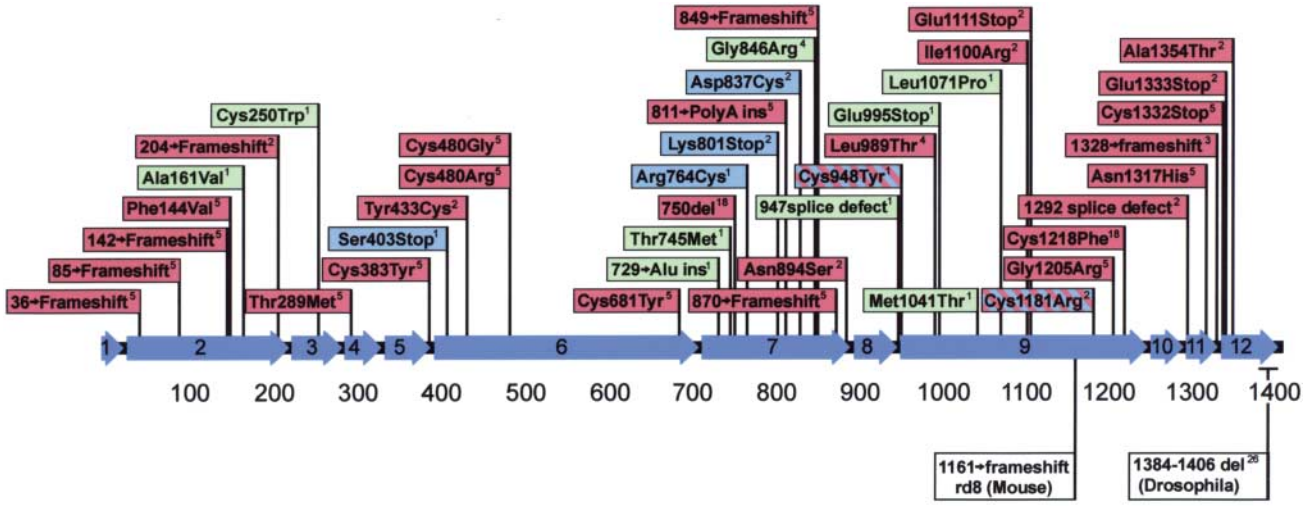

Figure 9. Schematic describing mutations in *Crb1*^{rd8} and *Drosophila* (26) relative to nucleotide alterations found in individuals with *Crb1* mutations (1,2,4,5,18). *Crb1* sequence variation observed in LCA patients (red), in RP (green), in RP with Coats exudative vasculopathy (blue), and in both patients with LCA or RP with Coats-like exudates (striped).

ACKNOWLEDGEMENTS

We are grateful to Wanda Hicks for her expert animal care, Elaine Gifford for her technical assistance, Jennifer Smith for graphics expertise, and Dr Susan L. Ackerman and Beverly Richards-Smith for careful review of this manuscript. Antibodies for PALS1 were generously provided by Dr B. Margolis. This work was supported by grants from the National Eye Institute, EY11996 and EY007758, the Macula Vision Research Foundation and the National Institute of Child Health and Human Development HD23839. Institutional shared services are supported by National Cancer Institute Cancer Center grant, CA-34196.

REFERENCES

1. Den Hollander, A.I., ten Brink, J.B., de Kok, Y.J., van Soest, S., van den Born, L.I., van Driel, M.A., van de Pol, D.J., Payne, A.M., Bhattacharya, S.S., Kellner, U. *et al.* (1999) Mutations in a human homologue of *Drosophila* crumbs cause retinitis pigmentosa (RP12). *Nat. Genet.*, **23**, 217–221.
2. Den Hollander, A.I., Heckenlively, J.R., van den Born, L.I., de Kok, Y.J., van der Velde-Visser, S.D., Kellner, U., Jurklies, B., van Schooneveld, M.J., Blankenagel, A., Rohrschneider, K. *et al.* (2001) Leber congenital amaurosis and retinitis pigmentosa with Coats-like exudative vasculopathy are associated with mutations in the crumbs homologue 1 (CRB1) gene. *Am. J. Hum. Genet.*, **69**, 198–203.
3. Gerber, S., Perrault, I., Hanein, S., Shalev, S., Zlotogora, J., Barbet, F., Ducroq, D., Dufier, J., Munnich, A., Rozet, J. *et al.* (2002) A novel mutation disrupting the cytoplasmic domain of CRB1 in a large consanguineous family of Palestinian origin affected with Leber congenital amaurosis. *Ophthal. Genet.*, **23**, 225–235.
4. Khaliq, S., Abid, A., Hameed, A., Anwar, K., Mohyuddin, A., Azmat, Z., Shami, S.A., Ismail, M. and Mehdi, S.Q. (2003) Mutation screening of Pakistani families with congenital eye disorders. *Exp. Eye Res.*, **76**, 343–348.
5. Lotery, A.J., Jacobson, S.G., Fishman, G.A., Weleber, R.G., Fulton, A.B., Namperumalsamy, P., Heon, E., Levin, A.V., Grover, S., Rosenow, J.R. *et al.* (2001) Mutations in the CRB1 gene cause Leber congenital amaurosis. *Arch. Ophthal.*, **119**, 415–420.
6. Tepass, U., Tanentzapf, G., Ward, R. and Fehon, R. (2001) Epithelial cell polarity and cell junctions in *Drosophila. A. Rev. Genet.*, **35**, 747–784.
7. Pellikka, M., Tanentzapf, G., Pinto, M., Smith, C., McGlade, C.J., Ready, D.F. and Tepass, U. (2002) Crumbs, the *Drosophil*a homologue of human CRB1/RP12, is essential for photoreceptor morphogenesis. *Nature*, **416**, 143–149.
8. Izaddoost, S., Nam, S.C., Bhat, M.A., Bellen, H.J. and Choi, K.W. (2002) *Drosophila* Crumbs is a positional cue in photoreceptor adherens junctions and rhabdomeres. *Nature*, **416**, 178–183.
9. Johnson, K., Grawe, F., Grzeschik, N. and Knust, E. (2002) *Drosophila* crumbs is required to inhibit light-induced photoreceptor degeneration. *Curr. Biol.*, **12**, 1675–1680.
10. Paffenholz, R., Kuhn, C., Grund, C., Stehr, S. and Franke, W.W. (1999) The arm-repeat protein NPRAP (neurojungin) is a constituent of the plaques of the outer limiting zone in the retina, defining a novel type of adhering junction. *Exp. Cell Res.*, **250**, 452–464.
11. Smith, R.S., Kao, W.-Y. and John, S.W.M. (2002) *Ocular Development, in Systematic Evaluation of the Mouse Eye*. CRC Press, Boca Raton, FL.
12. Bachmann, A., Schneider, M., Theilenberg, E., Grawe, F. and Knust, E. (2001) *Drosophila* Stardust is a partner of Crumbs in the control of epithelial cell polarity. *Nature*, **414**, 638–643.
13. Hong, Y., Stronach, B., Perrimon, N., Jan, L.Y. and Jan, Y.N. (2001) *Drosophila* Stardust interacts with Crumbs to control polarity of epithelia but not neuroblasts. *Nature*, **414**, 634–638.
14. Roh, M.H., Makarova, O., Liu, C.J., Shin, K., Lee, S., Lawrinec, S., Goyal, M., Wiggins, R. and Margolis, B. (2002) The Maguk protein, Pals1, functions as an adapter, linking mammalian homologues of Crumbs and Discs Lost. *J. Cell Biol.*, **157**, 161–172.
15. Hawes, N.L., Chang, B., Hageman, G.S., Nusinowitz, S., Nishina, P.M., Schneider, B.S., Smith, R.S., Roderick, T.H., Davisson, M.T. and Heckenlively, J.R. (2000) Retinal degeneration 6 (rd6): a new mouse model for human retinitis punctata albescens. *Invest. Ophthal. Visual Sci.*, **41**, 3149–3157.
16. Rich, K.A., Zhan, Y. and Blanks, J.C. (1997) Migration and synaptogenesis of cone photoreceptors in the developing mouse retina. *J. Comp. Neurol.*, **388**, 47–63.
17. Rich, K.A., Figueroa, S.L., Zhan, Y. and Blanks, J.C. (1995) Effects of Muller cell disruption on mouse photoreceptor cell development. *Exp. Eye Res.*, **61**, 235–248.
18. Jacobson, S.G., Cideciyan, A.V., Aleman, T.S., Pianta, M.J., Sumaroka, A., Schwartz, S.B., Smilko,E.E., Milam, A.H., Sheffield, V.C. and Stone, E.M. (2003) Crumbs homolog 1 (CRB1) mutations result in a thick human retina with abnormal lamination. *Hum. Mol. Genet.*, **12**, 1073–1078.
19. Gibson, F., Walsh, J., Mburu, P., Varela, A., Brown, K.A., Antonio, M., Beisel, K.W., Steel, K.P. and Brown, S.D. (1999) A type VII myosin encoded by the mouse deafness gene shaker-1. *Nature*, **374**, 62–64.

20. Weil, D., Blanchard, S., Kaplan, J., Guilford, P., Gibson, F., Walsh, J., Mburu, P., Varela, A., Levilliers, J., Weston, M.D.*et al.* (1995) Defective myosin VIIA gene responsible for Usher syndrome type 1B. *Nature*, **374**, 60–61.
21. El-Amraoui, A., Sahly, I., Picaud, S., Sahel. J., Abitbol, M. and Petit, C. (1996) Human Usher 1B/mouse shaker-1: the retinal phenotype discrepancy explained by the presence/absence of myosin VIIA in the photoreceptor cells. *Hum. Mol. Genet.*, **5**, 1171–1178.
22. Liu, X., Vansant, G., Udovichenko, I.P., Wolfrum, U. and William, D.S. (1999) Myosin VIIa participates in opsin transport through the photoreceptor cilium. *J. Neurosci.*, **19**, 6267–6274.
23. Buffone, G.J. and Darlington, G.J. (1985) Isolation of DNA from biological specimens without extraction with phenol. *Clin. Chem.*, **31**, 164–165.
24. Maddatu, T. and Naggert, J.K. (1997) Allele-specific PCR assays for the tub and cpefat mutations. *Mamm. Genome,***8**, 857–858.
25. den Hollander, A.I., Ghiani, M., de Kok, Y.J., Wijnholds, J., Ballabio, A., Cremers, F.P. and Broccoli, V. (2002) Isolation of Crb1, a mouse homologue of *Drosophila* crumbs, and analysis of its expression pattern in eye and brain. *Mech. Dev.,* **110**, 203–207.
26. Wodarz, A., Grawe, F. and Knust E. (1993) CRUMBS is involved in the control of apical protein targeting during *Drosophila* epithelial development. *Mech. Dev.*, **44**, 175–187.